Repression of Viral Gene Expression and Replication by the Unfolded Protein Response Effector XBP1u

Florian Hinte[1], Eelco van Anken[2,3], Boaz Tirosh[4], Wolfram Brune[1,*]

1 Heinrich Pette Institute, Leibniz Institute for Experimental Virology, Hamburg, Germany
2 Division of Genetics and Cell Biology, San Raffaele Scientific Institute, Milan, Italy
3 Università Vita-Salute San Raffaele, Milan, Italy
4 Institute for Drug Research, School of Pharmacy, Faculty of Medicine, The Hebrew University, Jerusalem, Israel
* Corresponding author. Phone: +49 40 48051351; Email: wolfram.brune@leibniz-hpi.de

Running title: Cytomegalovirus repression by XBP1u

Word count
Abstract: 165
Text: 4969

Abstract

The unfolded protein response (UPR) is a cellular homeostatic circuit regulating protein synthesis and processing in the ER by three ER-to-nucleus signaling pathways. One pathway is triggered by the inositol-requiring enzyme 1 (IRE1), which splices the X-box binding protein 1 (XBP1) mRNA, thereby enabling expression of XBP1s. Another UPR pathway activates the activating transcription factor 6 (ATF6). Here we show that murine cytomegalovirus (MCMV), a prototypic β-herpesvirus, harnesses the UPR to regulate its own life cycle. MCMV activates the IRE1-XBP1 pathway early post infection to relieve repression by XBP1u, the product of the unspliced XBP1 mRNA. XBP1u inhibits viral gene expression and replication by blocking the activation of the viral major immediate-early promoter by XBP1s and ATF6. These findings reveal a redundant function of XBP1s and ATF6 as activators of the viral life cycle, and an unexpected role of XBP1u as a potent repressor of both XBP1s and ATF6-mediated activation.

Key words: unfolded protein response / transcription factor / XBP1u / ATF6 / cytomegalovirus.

Introduction

The endoplasmic reticulum (ER) is responsible for synthesis, posttranslational modification, and folding of a substantial portion of cellular proteins. When protein synthesis is increased or ER function is compromised, the folding capacity of the ER may get out of balance, leading to an accumulation of unfolded or misfolded proteins in the ER. To alleviate ER stress and restore homeostasis, the cell activates three ER-to-nucleus signaling pathways, collectively called the unfolded protein response (UPR), which lead to a reduced protein synthesis and an increased expression of folding chaperones and ER-associated degradation (ERAD) factors (Walter & Ron, 2011). Subsequently, ER folding capacity increases and terminally misfolded protein species are exported from the ER and targeted for proteasomal degradation (Christianson & Ye, 2014).

In mammalian cells, the UPR comprises three main signaling pathways named after the initiating ER stress sensors: PERK (PKR-like ER kinase), ATF6 (activating transcription factor 6), and IRE1 (inositol-requiring enzyme 1) (Walter & Ron, 2011). Upon activation by ER stress, PERK phosphorylates the translation initiation factor eIF2α, which leads to a massive attenuation of protein synthesis and an immediate reduction of the protein load in the secretory system. However, phosphorylated eIF2α selectively supports the translation of selected cellular proteins such as the transcription factor ATF4, which activates a negative feedback loop resulting in dephosphorylation of eIF2α (Novoa et al, 2001).

Upon activation by ER stress, ATF6 travels to the Golgi, where it undergoes intramembrane proteolysis. This process liberates its cytosolic N-terminus, the basic leucine zipper (bZIP) transcription factor ATF6(N), and enables it to travel to the nucleus, where it activates the transcription of chaperone genes as well as of the gene encoding XBP1 (Lee et al, 2002).

The third sensor, IRE1, is an ER transmembrane protein kinase that oligomerizes upon accumulation of unfolded proteins in the ER lumen. Oligomerization and auto-transphosphorylation activates the RNase function of IRE1, which mediates an unconventional splicing of the XBP1 mRNA in the cytosol (Calfon et al, 2002; Lee et al, 2002; Yoshida et al, 2001). Removal of the 26-nt intron from the XBP1 mRNA leads to a frame shift and expression of transcription factor XBP1s, comprising an N-terminal basic leucine zipper (bZIP) domain followed by a C-terminal transcription activation domain. In contrast, the unspliced XBP1 mRNA encodes XBP1u, which lacks the transcription activation domain but contains a hydrophobic patch in the C-terminal part. XBP1u is rapidly degraded and has a short half-life (Tirosh et al, 2006). It can interact with XBP1s and ATF6(N) and target them for proteasomal degradation. Therefore, XBP1u is thought acts as a negative regulator involved in fine-tuning the UPR (Tirosh et al, 2006; Yoshida et al, 2006; Yoshida et al, 2009). Moreover, XBP1u affects autophagy by interacting with transcription factor FOXO1 (Zhao et al, 2013). Apart from mediating XBP1 mRNA splicing, IRE1 can also cleave ER-associated mRNA molecules that contain a specific recognition motif (Moore & Hollien, 2015). This process, which leads to mRNA degradation, is called regulated IRE1-dependent mRNA decay (RIDD). However, the importance of RIDD in different cellular processes such as lipid metabolism, antigen presentation, and apoptosis remains incompletely understood (Maurel et al, 2014).

During viral replication large quantities of viral proteins must be synthesized. Folding, maturation, and posttranslational modification of secreted and transmembrane proteins take place in the ER and require a plethora of chaperones, foldases, and glycosylating enzymes. While properly folded proteins are transported to the Golgi, unfolded or misfolded proteins are retained in the ER and exported to the cytosol for proteasomal degradation via the ER-associated protein degradation (ERAD) pathway (Smith et al, 2011). However, the high levels of viral envelope glycoproteins that are being synthesized particularly during the late phase of the viral life cycle can overwhelm the folding and processing capacity of the ER and cause accumulation of unfolded and misfolded proteins in the ER (Zhang & Wang, 2012).

Cytomegaloviruses (CMVs) are prototypic members of the β subfamily of the *Herpesviridae*. Their large double-stranded DNA genomes contain at least 165 protein-coding ORFs (Dolan et al, 2004) end encode an even larger number of polypeptides (Stern-Ginossar et al, 2012). Through millions of years of co-evolution with their respective hosts,

75 the CMVs have acquired the ability to moderate immune recognition and modulate cellular
76 stress responses to their own benefit (Alwine, 2008; Mocarski, 2002). Considering the
77 important role of the UPR in controlling cell fitness, it is hardly surprising that the CMVs have
78 evolved means to modify the UPR. For instance, human and murine CMV (HCMV and
79 MCMV) induce PERK activation, but limit eIF2α phosphorylation. By doing this the CMVs
80 prevent a global protein synthesis shutoff but allow eIF2α phosphorylation-dependent
81 activation of transcription factor ATF4 (Isler et al, 2005; Qian et al, 2012). The CMVs also
82 increase expression of the ER chaperone BiP to facilitate protein folding and virion assembly
83 (Buchkovich et al, 2008; Buchkovich et al, 2010; Qian et al, 2012), and HCMV uses PERK to
84 induce lipogenesis by activating the cleavage of sterol regulatory element binding protein 1
85 (Yu et al, 2013). We have previously shown that both, MCMV and HCMV, downregulate
86 IRE1 levels and inhibit IRE1 signaling at late times post infection. This downregulation is
87 mediated by the viral proteins M50 and UL50, respectively (Stahl et al, 2013). However, a
88 real-time transcriptional profiling study has revealed that cellular ER stress response
89 transcripts are upregulated as early 5-6 hours after MCMV infection (Marcinowski et al,
90 2012).
91 Here we show that MCMV transiently activates the IRE1-XBP1 pathway at early times
92 postinfection in order to relieve repression of viral gene expression and replication by XBP1u.
93 When IRE1-mediated XBP1 mRNA splicing is inhibited, XBP1u blocks the activation of the
94 viral major immediate-early promoter (MIEP) by XBP1s and ATF6(N). Thus, MCMV exploits
95 UPR signaling to boost the activity of its most important promoter. Moreover, these findings
96 reveal a redundant function of XBP1s and ATF6 as activators of viral gene expression and
97 replication, and an unexpected role of XBP1u as a potent repressor of both XBP1s and
98 ATF6-mediated activation.
99

100 ## Results

101 **Early activation of IRE1-XBP1 signaling promotes MCMV replication.**

102 Previous studies have shown that MCMV inhibits IRE1-XBP1 signaling at late times (≥24 h)
103 post infection (Qian et al, 2012; Stahl et al, 2013). However, cellular ER stress response
104 transcripts were shown to be upregulated at 5-6 hours after MCMV infection (Marcinowski et
105 al, 2012), suggesting that UPR signaling is activated at early times post infection. Thus, we
106 decided to analyze whether MCMV activates the IRE1-XPB1 signaling pathway within the
107 first few hours after infection. To do this, we infected mouse embryonic fibroblasts (MEFs)
108 with MCMV and quantified spliced and unspliced XBP1 transcripts by qRT-PCR. We
109 detected a short and transient increase of XBP1 splicing between 5 and 7 hours post
110 infection (hpi) (Fig. 1A). This increase was massively reduced when cells were infected with
111 UV-inactivated MCMV (Fig. 1A), suggesting that XBP1 splicing was not caused by viral

112 attachment and entry into cells but required viral gene expression. MCMV-induced XBP1
113 splicing was also suppressed by cycloheximide (CHX, a translation inhibitor), but not by
114 phosphonoacetic acid (PAA), an inhibitor of viral DNA replication and late gene expression
115 (Fig. 1B). These results suggested that the transient activation of the IRE1-XBP1 pathway is
116 caused by viral proteins expressed at immediate-early or early times post infection.

117 To determine whether IRE1 signaling is important for the MCMV life cycle, we used
118 *Ire1*$^{-/-}$ cells expressing IRE1-GFP under tight control of a tetracycline-inducible promoter (Fig.
119 2A) for analyses of viral replication. IRE1-GFP expression was induced with different
120 concentrations of doxycycline, and cells were infected at low or high multiplicity of infection
121 (MOI) for multi-step and single-step growth curves, respectively (Fig. 2B and C). In both
122 types of replication analysis, MCMV replicated to low titers when IRE1 expression was
123 induced with very low or very high doxycycline concentrations. High MCMV titers (~10^6
124 infectious units per ml), comparable to those obtained in wildtype (WT) MEFs, were attained
125 only upon moderate induction of IRE1-GFP with 5 to 10 nM doxycycline (Fig. 2B and C).
126 Thus we concluded that IRE1 is necessary for efficient replication of MCMV, but needs to be
127 carefully regulated as too high expression levels are detrimental for viral replication.
128

129 **IRE1, but not XBP1 or TRAF2, is required for efficient MCMV gene expression and**
130 **replication.**

131 Activated IRE1 can splice *Xbp1* mRNA (Calfon et al, 2002; Lee et al, 2002; Yoshida et al,
132 2001) and can also recruit TRAF2 to activate ASK1 (Urano et al, 2000). To test which IRE1-
133 dependent signaling pathway is required for efficient MCMV replication, we used
134 CRISPR/Cas9-mediated gene editing to generate *Ire1* knockout (ko), *Xbp1* ko, and *Traf2* ko
135 MEFs. For each gene knockout, two independent cell clones were generated with different
136 guide RNAs. The absence of the respective gene products was verified by immunoblot
137 analysis (Fig. 3A). Then the cell clones were used to assess MCMV replication. In *Ire1* ko
138 MEFs, viral replication was reduced by two orders of magnitude as compared to WT MEFs
139 (Fig. 3B), similar to the reduction seen in IRE1-GFP cells without doxycycline induction (Fig.
140 2B). By contrast, MCMV replication was virtually unimpaired in the absence of *Xbp1* (Fig. 3B)
141 or *Traf2* (Fig. 3C). We also analyzed the expression of a viral immediate-early (IE1), an early
142 (M57), and a late protein (gB) at different times post infection. Compared to WT MEFs, the
143 expression of all three proteins was reduced in *Ire1* ko MEFs (Fig. 3D), but not in *Xbp1* or
144 *Traf2* ko MEFs (Fig. 3E and F).

145 Next we tested whether the RNAse activity of IRE1 is required for efficient MCMV
146 replication. To do this, WT IRE1 or an "RNAse-dead" IRE1 K907A mutant (Tirasophon et al,
147 2000) was expressed in *Ire1* ko MEFs by retroviral transduction. Expression of WT and
148 mutant IRE1 and the ability to splice *Xbp1* was verified by immunoblot analysis (Fig. 4A).

149 While expression of WT IRE1 restored MCMV replication to high titers, expression of IRE1
150 K907A did not increase MCMV titers (Fig. 4B), indicating that the IRE1 RNase activity is
151 necessary for efficient MCMV replication.
152
153 **XBP1u inhibits MCMV replication.**
154 Our observations that the RNase activity of IRE1 is required for efficient MCMV replication,
155 but XBP1 is not, allowed two possible explanations: (i) MCMV replication could benefit from
156 RIDD, another RNase-dependent function of IRE1. However, this possibility is difficult to
157 verify as selective inactivation of RIDD is complicated. (ii) Alternatively, MCMV replication
158 could be inhibited by XBP1u, the product of the unspliced *Xbp1* mRNA, since *Ire1* ko cells
159 differ from other cells in that they express only XBP1u (Fig. 3A). To test the latter option, we
160 used two experimental approaches. First, we knocked out *Ire1* in *Xbp1*-deficient cells (Fig.
161 5A). As shown in figure 5B, MCMV replicated to similar titers in *Xbp1* ko and *Xbp1*/*Ire1*
162 double-knockout (dko) cells, indicating that the loss of IRE1 is not detrimental for MCMV
163 replication when XBP1 is absent. Next, we used retroviral transduction to restore XBP1
164 expression in *Xbp1*$^{-/-}$ cells. The retroviral vectors expressed the WT *Xbp1* transcript (which
165 can be spliced by IRE1), a truncated *Xbp1* transcript encoding only the DNA-binding domain,
166 or an 'unspliceable' *Xbp1* transcript. Upon treatment with thapsigargin, these cells expressed
167 XBP1s, XBP1stop, or XBP1u, respectively (Fig. 5C). Whereas re-introduction of WT XBP1
168 had no detrimental effect, MCMV replication was severely impaired upon expression of the
169 unspliceable *Xbp1* transcript (Fig. 5D), indicating that *Xbp1u* reduces viral replication. A
170 similar inhibitory effect was observed when the truncated XBP1 (XBP1stop) protein was
171 expressed (Fig. 5D).
172
173 **Loss of XBP1 and ATF6 impairs MCMV replication.**
174 XBP1u is thought to function as a negative regulator to XBP1s (Tirosh et al, 2006; Yoshida et
175 al, 2006). However, the inhibition of MCMV replication by XBP1u cannot be explained solely
176 by a repressive effect on XBP1s as a complete loss of XBP1 is not detrimental to MCMV
177 replication in vitro (Fig. 3B) and has only a modest effect on viral replication in vivo (Drori et
178 al, 2014). Thus we hypothesized that XBP1u might impair MCMV replication by repressing
179 the activity of additional transcription factors besides XBP1s. For several reasons ATF6
180 appeared to be a likely target of XBP1u: (i) Like XBP1s, ATF6 is a bZIP transcription factor
181 activated by ER stress (Yoshida et al, 1998); (ii) XBP1s and ATF6 are known to synergize in
182 the activation of numerous ER stress response genes (Lee et al, 2002); and (iii) XBP1u can
183 interact with ATF6 and inhibit its activity (Yoshida et al, 2009). Therefore, we tested whether
184 the loss of both, XBP1 and ATF6, was detrimental for MCMV replication. First, we analyzed
185 MEFs from *Atf6*$^{-/-}$ mice and found that MCMV gene expression and replication were not

186 impaired (Fig. 6A and B). When we knocked out *Xbp1* in *Atf6*$^{-/-}$ cells by CRISPR/Cas9 gene
187 editing (Fig. 6C), MCMV replication was substantially reduced in *Atf6*/*Xbp1* dko cells (Fig.
188 6D), suggesting that ATF6 and XBP1s have overlapping or redundant functions and that at
189 least one of them is necessary for efficient MCMV replication.
190
191 **XBP1s and ATF6-mediated activation of the MCMV major immediate-early promoter**
192 **(MIEP) is repressed by XBP1u.**
193 The MCMV MIEP has a key role in viral gene expression as it drives the expression of the
194 viral IE1 and IE3 proteins. IE3 is the major transactivator protein that activates early and late
195 gene expression (Lacaze et al, 2011). Thus we interrogated whether XBP1s and ATF6 can
196 activate the MCMV MIEP. First, we searched for ACGT motifs within the MCMV MIEP. ACGT
197 is a minimal consensus sequence contained within XBP1s and ATF6 binding motifs
198 (Kanemoto et al, 2005; Wang et al, 2000). Five ACGT motifs were identified within the
199 MCMV MIEP (Fig. 7A). To analyze the function of these putative transcription factor binding
200 sites, we inserted the WT MIEP and six mutant versions (Table S1) into the luciferase
201 reporter plasmid pGL3-Basic. In the mutant MIEPs, one or all five ACGT motifs were
202 changed to CTAG. Using a luciferase reporter assay, we measured MIEP activity in WT, *Ire1*
203 ko and *Xbp1* ko fibroblasts. As shown in Fig. 7B, MIEP activity was strongly reduced in *Ire1*
204 ko cell but was not significantly altered in *Xbp1* ko cells. This result is consistent with the
205 MCMV replication defect observed in *Ire1*, but not *Xbp1* ko cells (Fig. 3B). MIEP activity was
206 not reduced in *Xbp1*/*Ire1* dko cells compared to the parental *Xbp1* ko cell (Fig. 7C), but was
207 significantly reduced in *Atf6*/*Xbp1* dko cells compared to the parental *Atf6* ko cells (Fig. 7D).
208 Again, the MIEP activities were consistent with the results of the viral replication kinetics
209 (Figs. 5B and 6D). Thus, we concluded that activation of the MCMV MIEP correlated with
210 viral replication in the same cells. We also found that the activity of the MIEP had a
211 substantially reduced activity when all 5 ACGT motifs were mutated (Fig. 7B-D).
212 Next we tested whether XBP1s and ATF6(N), the active form of ATF6, can activate
213 the MCMV MIEP and whether XBP1u can repress it. To assess the contribution of
214 endogenous levels of the TFs, *Xbp1* ko, *Atf6* ko, and *Xbp1*/*Atf6* dko cells were used. In *Xbp1*
215 ko cells, MIEP activity was slightly increased by expression of XBP1s, but substantially
216 reduced by XBP1u. XBP1u also antagonized XBP1s in a dose-dependent manner (Fig. 7E).
217 A similar result was obtained in *Atf6*$^{-/-}$ cells: MIEP activity was slightly increased by
218 expression of ATF6(N), but substantially reduced by XBP1u. XBP1u also antagonized
219 ATF6(N) in a dose-dependent manner (Fig. 7F). In *Atf6*/*Xbp1* dko cell, expression of either
220 XBP1s or ATF6(N) was sufficient to increase MIEP activity substantially. XBP1u alone did
221 not reduce MIEP activity in these cells, but it antagonized the activity of ATF6(N) expressed
222 by transfection (Fig. 7G). Taken together, these results suggest that both, XBP1s and

223 ATF6(N), can activate the MCMV MIEP in a largely redundant fashion, and that XBP1u
224 represses the activity of both, XBP1s and ATF6(N).
225
226 **Motif 4 is necessary and sufficient for MIEP activation by XBP1s and ATF6(N).**
227 As a first step to determine, which of the five ACGT motifs function as XBP1s and/or
228 ATF6(N) binding sites for promoter activation, we measured the binding of these TFs to
229 portions of the MIEP by using a DNA-protein interaction ELISA (DPI-ELISA, (Brand et al,
230 2010; Underwood et al, 2013). Microtiter plates were coated with double-stranded
231 oligonucleotides encoding three copies (27 nucleotides each) of a putative binding motif with
232 adjacent sequences on either side (Table S3). A known XBP1 binding motif of the ERdj4
233 promoter (Kanemoto et al, 2005) served as positive control and a sequence of the SV40
234 origin of replication as negative control. The oligonucleotides were incubated with HA-tagged
235 XBP1s, XBP1u, or ATF6(N) (Fig. 8A), and DNA binding was quantified by ELISA. Mutated
236 TFs lacking the DNA-binding domain (ΔDBD) served as negative controls. In this DPI-ELISA,
237 XBP1s and XBP1u showed the strongest interaction with motifs 3 and 4, whereas ATF6(N)
238 interacted with motifs 2 and 4 (Fig. 8B).
239 Next we used the luciferase reporter assay to test which of the five motifs was
240 required for MIEP activation by XBP1s and ATF6(N). We used five mutant MIEPs having one
241 of the ACGT motifs changed to CTAG. These reporter plasmids were transfected into
242 *Atf6*/*Xbp1* dko cells, together with expression plasmids for XBP1s, XBP1u, and ATF6(N). As
243 shown in Fig. 9A, XBP1s or ATF6(N) expression increased the activity of all MIEP constructs
244 except MIEP-4-mut and MIEP-all-mut, indicating that ACGT motif 4 is necessary for MIEP
245 activation by XBP1s and ATF6(N).
246 We tested then whether motif 4 was also sufficient for MIEP activation by XBP1s and
247 ATF6(N). Motif 4 was restored in MIEP-all-mut to generate a MIEP containing only ACGT
248 motif 4 (MIEP-4-only, Table S1). Indeed, MIEP-4-only was inducible by XBP1s and ATF6(N)
249 (Fig. 9B), suggesting that motif 4 is sufficient to confer MIEP responsiveness to XBP1s and
250 ATF6. To determine whether motif 4 is also of crucial importance for MCMV replication, we
251 mutated motif 4 within the MCMV genome. The resulting virus, MCMV-GFP-4-mut, was
252 compared to the parental MCMV-GFP virus in a multi-step replication kinetic analysis (Fig.
253 9C). Indeed, viral replication was massively reduced when motif 4 within the MIEP was
254 mutated. This result confirmed that the XBP1 and ATF6(N) target motif identified in DNA-
255 binding and luciferase reporter assays is required for efficient replication of the virus.
256 Taken together, the results of this study show that MCMV transiently activates the
257 IRE1-XBP1 signaling pathway in the early phase of infection in order to relieve XBP1u-
258 mediated repression of viral gene expression and replication. The MCMV major immediate-
259 early promoter requires XBP1s or ATF6(N) binding to motif 4 for full activation, and XBP1u

260 prevents promoter activity by both TFs. Thus, XBP1u acts as a key repressor of two UPR
261 pathways, the IRE1-XBP1 and the ATF6 pathways, which have overlapping and redundant
262 functions.
263

264 **Discussion**

265 This study shows how MCMV harnesses UPR signaling to regulate its own life cycle. The
266 viral MIEP, the key promotor of the lytic replication cycle, contains five ACGT motifs, of which
267 motif 4 is most important for MIEP activation by XBP1s or ATF6(N) (Fig. 9). The fact that
268 MIEP activity and viral replication are virtually unaffected in the absence of either XBP1 or
269 ATF6 but are massively reduced in the absence of both, strongly suggests that the two UPR
270 TFs have redundant roles in the activation of the MIEP. The most important finding, however,
271 is the dominant role of XBP1u as a repressor of viral gene expression and replication. When
272 IRE1 is absent or its RNase activity is blocked, XBP1u dominates and prevents MIEP
273 activation by XBP1s and ATF6(N). Thus, the transient activation of IRE1 during the early
274 phase of MCMV infection serves the virus by increasing XBP1s and decreasing XBP1u
275 expression, thereby relieving XPB1u-mediated repression.

276 How exactly XBP1u antagonizes XBP1s and ATF6(N)-mediated promoter activation,
277 remains to be determined. Two possible mechanisms may be involved: XBP1u could interact
278 with XBP1s and ATF6(N) and target them for proteasomal degradation as previously
279 reported (Yoshida et al, 2006; Yoshida et al, 2009). Additionally, XBP1u could bind directly to
280 DNA and inhibit promoter activation by XBP1s and ATF6(N). Indeed, we show that XBP1u is
281 fully capable of binding to the same DNA sequences that XBP1s binds to (Fig. 8). Moreover,
282 a truncated XBP1 protein, XBP1stop, which lacks the C-terminal destabilizing domain of
283 XBP1u, had a similar repressive effect as XBP1u (Fig 5D) indicating that destabilization is
284 not required for repression.

285 Ever since its discovery, the importance of XBP1u has been the subject of
286 controversy. In yeast, the unspliced mRNA of HAC1, the yeast homolog of XBP1, is
287 posttranscriptionally silenced, and a protein product of the unspliced HAC1 mRNA has not
288 been detected (Ruegsegger et al, 2001). In mammalian cells, the XBP1u protein is readily
289 detectable, but XBP1u has a short half-life (Navon et al, 2010; Tirosh et al, 2006). This has
290 led to the conclusion that XBP1u is of minor importance and its function restricted to fine-
291 tuning of the UPR (Byrd & Brewer, 2012). Hence, many review articles on the UPR barely
292 mention XBP1u. On the other hand, XBP1u has been shown to dimerize with XBP1s and
293 ATF6(N) and destabilize them (Yoshida et al, 2006; Yoshida et al, 2009), suggesting a more
294 important regulatory role. However, the physiological relevance of these findings has been
295 called into question by some scientists because the findings were made in cells
296 overexpressing XBP1u. The results of our study show that XBP1u plays a very important role

297 as a repressor of XBP1s and ATF6(N)-mediated activation of the MCMV MIEP, which results
298 in a massively (~100-fold) reduced production of progeny virus (Figs. 2, 3B, and 5D). In IRE1
299 ko cells, the XBP1 transcript is expressed from its endogenous promoter, not from a strong
300 heterologous promoter. Thus, the observed effects cannot be dismissed as overexpression
301 artifacts. Moreover, the fact that MCMV replication is massively reduced in IRE1 ko cells
302 (Figs. 2 and 3B), but not in *Ire1*/*Xbp1* dko cells (Fig. 5B), demonstrates that XBP1u
303 expression rather than the absence RIDD is responsible for the observed effect. Hence, the
304 data of our study suggest that XBP1u plays an unexpectedly important role as a repressor, at
305 least under the conditions of viral infection. Whether XBP1u can repress expression of
306 cellular genes in a similar fashion is an important question that needs to be answered in
307 future studies.

308 XBP1 binding sites have also been identified in immediate-early gene promoters of
309 the γ-herpesviruses Epstein-Barr virus, Kaposi's sarcoma-associated herpesvirus, and
310 murine gammaherpesvirus 68 (MHV-68), suggesting a potential role for XBP1s in
311 transactivating these promoters during reactivation from latency (Bhende et al, 2007; Matar
312 et al, 2014; Sun & Thorley-Lawson, 2007; Wilson et al, 2007; Yu et al, 2007). However, one
313 study demonstrated that XBP1 was not required for MHV-68 reactivation in B cells (Matar et
314 al, 2014). The authors of the study speculated that the apparent independence of MHV-68
315 reactivation from XBP1 expression in B cells might reflect redundancy among CREB/ATF
316 family TFs. In light of our data showing a redundancy of XBP1s and ATF6(N) in the activation
317 of the MCMV MIEP, this conjecture may well be correct. Conversely, it would be interesting
318 to know whether XBP1 and ATF6 also regulate MCMV reactivation from latency.
319 Unfortunately, this obvious question is difficult to address as there is no manageable cell
320 culture system for MCMV latency and reactivation. Nonetheless, it appears likely that β and
321 γ-herpesviruses harness UPR TFs in a similar fashion to regulate their life cycle.
322

323 ## Materials and Methods

324 ### Cells and viruses

325 The following immortalized fibroblast lines were used: wildtype MEFs (Manzl et al, 2009),
326 10.1 cells (Harvey & Levine, 1991), *Xbp1*$^{-/-}$ MEFs (Reimold et al, 2000), Primary *Atf6*$^{+/+}$ and
327 *Atf6*$^{-/-}$ MEFs (Wu et al, 2007) were kindly provided by D. Thomas Rutkowski (University of
328 Iowa, USA). They were immortalized by transduction with a retroviral vector encoding SV40
329 large T antigen (pBABE-zeo largeTcDNA, Addgene). The *Atf6*$^{+/+}$ vs. *Atf6*$^{-/-}$ state was verified
330 by PCR as described (Wu et al, 2007). TetON-IRE1-GFP MEFs were obtained by
331 reconstituting *Ire1*$^{-/-}$ MEFs with GFP-tagged murine IRE1 under control of a 'tight' Tet-
332 responsive element (Clontech) essentially as described (Bakunts et al, 2017; Cohen et al,
333 2017). The GFP tag was introduced into the juxtamembrane cytosolic linker domain of IRE1,

334 where such tagging had been shown before to not interfere with function of human IRE1 (Li
335 et al, 2010). All cells were grown under standard conditions in Dulbecco´s modified Eagle´s
336 medium supplemented with 10% fetal calf serum or 10% fetal calf serum tetracycline-free,
337 100 IU/ml penicillin and 100 µg/ml streptomycin (Sigma).
338 MCMV-GFP (Brune et al, 2001) was propagated and titrated on 10.1 fibroblasts. Viral
339 titers were determined by using the median tissue culture infective dose ($TCID_{50}$) method.
340 Virus was inactivated by 254-nm-wavelength UV irradiation with 1 J/cm^2 for 30 s using a UV
341 cross-linker (HL-2000 HybriLinker; UVP).
342
343 **Mutagenesis of the MCMV MIEP**
344 The recombinant MCMV carrying an ACGT-to-CTAG mutation of MIEP motif 4 was
345 constructed by BAC (bacterial artificial chromosome) recombineering using the *en passant*
346 mutagenesis protocol (Tischer et al., 2010). A kanamycin resistant gene was PCR-amplified
347 using primers MIEP_4_mut fwd (5'-GGTACTTTCCCATAGCTGATTAATGGGAA-
348 AGTACCGTTCTCGAGCCAATAC*CTAG*CAATGGGAAGTGAAAGGGCAGtagggataacagggta
349 atcgattt-3') and MIEP_4-mut rev (5'-GGGGAAAACCGGGGCGGTGTTACGTTTTGG-
350 CTGCCCTTTCACTTCCCATTG*CTAG*GTATTGGCTCGAGAACGGTACTgccagtgttacaaccaat
351 taacc-3'). The linear PCR product was used for homologous recombination in *Escherichia*
352 *coli* strain GS1783 containing the MCMV-GFP BAC. The kanamycin resistance cassette was
353 used for positive selection in the first recombination step and removed in the second step
354 (Tischer et al., 2010). The MCMV-GFP-4-mut BAC was examined by restriction fragment
355 analysis and sequencing of the mutated region. Mutant and control viruses were
356 reconstituted by BAC transfection of mouse fibroblast using GenJet transfection reagent
357 (SignaGen).
358
359 **Plasmids and transfection**
360 XBP1-wt and XBP1-unsplicable cDNAs (Tirosh et al, 2006) were cloned in pcDNA3. The
361 XBP1-wt vector was used to generate by PCR an XBP1stop mutant consisting of only the N-
362 terminal domain of XBP1. The XBP1s cDNA was generated by isolating RNA from MEFs
363 stimulated with tunicamycin (Sigma), reverse transcription, and PCR amplification. To
364 generate XBP1-unsplicable and XBP1-spliced plasmids lacking the DNA-binding domain
365 (ΔDBD) the complete DBD was replaced by an alternative NLS sequence as previously
366 described (Zhou et al, 2011). Transcripts of XBP1 proteins were HA-tagged by PCR
367 amplification and subcloned in pMSCVpuro (Clonetech), a retroviral vector plasmid. Similarly,
368 mIRE1-wt was PCR-amplified (without a myc tag) from pcDNA3-mIRE1-3xmyc (Stahl et al,
369 2013) and subcloned in pMSCVhyg (Clontech) using BglII and HpaI sites. The K907A

370 mutation was introduced by QuikChange site-directed mutagenesis (Stratagene). Transient
371 transfection was done using GenJet (SignaGen) or polyethylenimine (Sigma).
372
373 **Retroviral transduction and CRISPR/Cas9 gene editing**
374 Retrovirus production using the Phoenix packaging cell line and transduction of target cells
375 was done as described (Swift et al, 2001). Cells transduced with MSCVpuro and MSCVhyg
376 vectors were selected with 1.5 µg/ml puromycin (Sigma) or 50 µg/ml hygromycin B (Roth),
377 respectively.
378 Guide RNAs (Table S2) for genes of interest were designed using the online tool E-
379 CRISP (http://www.e-crisp.org/E-CRISP/designcrispr.html) and inserted into the lentiviral
380 vector pSicoR-CRISPR-puroR (kindly provided by R. J. Lebbink, University Medical Center
381 Utrecht, Netherlands). Lentiviruses were produced in 293T cells using standard third-
382 generation packaging vectors as described (van Diemen et al, 2016). Lentiviruses were used
383 to transduce MEFs in the presence of polybrene (5 µg/ml). Cells were selected with 1.5 µg/ml
384 puromycin and single cell clones were obtained by limiting dilution.
385
386 **Immunoblot analysis**
387 Whole cell lysates were obtained by lysing cells in RIPA buffer supplemented with a
388 cOmplete™, Mini protease inhibitor cocktail (Roche). XBP1s, XBP1u, and ATF6(N) were
389 extracted from cells treated with thapsigargin (Sigma) using a nuclear extraction protocol
390 (Stahl et al, 2013). Insoluble material was removed by centrifugation. Protein concentrations
391 were measured using a BCA assay (company). Equal protein amounts were boiled in sample
392 buffer and subjected to SDS-PAGE and semi-dry blotting onto nitrocellulose membranes. For
393 immunodetection, antibodies against the following epitopes were used: HA (16B12,
394 BioLegend), β-actin (AC-74, Sigma), XBP1 (M-186, Santa Cruz), IRE1 (14C10, Cell
395 Signaling), TRAF2 (Cell Signaling), and GFP (Roche). Antibodies against MCMV IE1
396 (CROMA101), M57, and M55/gB (SN1.07) were provided by Stipan Jonjic (University of
397 Rijeka, Croatia). Secondary antibodies coupled to horseradish peroxidase (HRP) were
398 purchased from Dako.
399
400 **RNA isolation and quantitative PCR**
401 Total RNA was isolated from MEFs using an innuPREP RNA Mini Kit (Analytik-Jena).
402 Reverse transcription and cDNA synthesis was carried out with 2 µg RNA using 200 U
403 RevertAid H Minus Reverse Transcriptase, 100 pmol Oligo$(dT)_{18}$, and 20 U RNase inhibitor
404 (Thermo Fisher Scientific). Quantitative real-time PCR reactions employing SYBR Green
405 were run in a 7900HT Fast Real-Time PCR System (Applied Biosystems). The following
406 primers were used: 5′-GAGTCCGCAGCAGGTG-3′ and 5′-GTGTCAGAGTCCATGGGA-3′ for

407 *Xbp1s*, 5′-GTGTCAGAGTCCATGGGA-3′ and 5′-GTGTCAGAGTCCATGGGA-3′ for X*bp1u,*
408 *and* 5′-CCCACTCTTCCACCTTCGATG-3′ and 5′-GTCCACCACCCTGTTGCTGTAG-3′ for
409 *Gapdh*. Reactions were performed under the following conditions: 45 cycles of 3 sec at 95°C
410 and 30 sec at 60°C. Three replicates were analyzed for each condition, and the relative
411 amounts of mRNAs were calculated from the comparative threshold cycle (Ct) values by
412 using *Gapdh* as reference.
413
414 **Replication kinetics**
415 Cells were seeded in 6-well plates and infected by an MOI of 3 or 0.1 for single or multi-step
416 replication kinetics, respectively. Six hpi the medium was exchanged to remove the
417 inoculum. Supernatant samples were harvested at different times post infection, and viral
418 titers were determined on 10.1 fibroblasts using the $TCID_{50}$ method.
419
420 **MIE promotor activity assay**
421 The firefly luciferase reporter vector pGL3-Basic, the renilla luciferase control vector
422 pGL4.73, and the Dual-Glo Luciferase assay system were purchased from Promega. WT
423 and mutant versions of the MCMV MIE promotor (Table S1) were synthesized by Integrated
424 DNA Technologies and cloned in pGL3-Basic. Cells were transfect in 6-well dishes using
425 GenJet with pGL3-MIEP (0.5 µg), pGL4.73 (0.05 µg) and transcription factor expression
426 plasmids. The total amount of DNA was kept constant at 3 µg by filling up with empty
427 pcDNA3 vector. On the following day, the medium was exchanged and cells were incubated
428 for another 24 h. Cells were harvested in lysis buffer and luciferase activity was measured
429 using a Dual-Glo Luciferase assay and a luminescence plate reader (FLUOstar-Omega,
430 BMG Labtech). Firefly and Renilla luciferase activities were evaluated for each sample. At
431 least 3 biological replicates were used for each condition.
432
433 **DNA-Protein Interaction ELISA (DPI-ELISA)**
434 The DPI-ELISA was performed essentially as described in detail elsewhere (Brand et al,
435 2010; Underwood et al, 2013). Terminally biotinylated dsDNA oligonucleotides containing 3
436 copies of putative TF binding sites (Table S3) were purchased from Eurofins.
437 Oligonucleotides were adsorbed to streptavidin-coated 96-well microtiter plates and
438 incubated with nuclear extracts (10 µg protein) from transfected HEK 293A cells expressing
439 the HA-tagged XBP1 or ATF6(N) proteins. Nuclear extracts were obtained as described
440 (Stahl et al, 2013). TF binding to DNA was quantified by ELISA using an anti-HA antibody, an
441 HRP-coupled secondary antibody, and an ABTS substrate (Roche). Absorbance at 405 nm
442 wavelength was measured using a FLUOstar-Omega plate reader. At least 3 biological
443 replicates were used for each condition.

444 **Statistical analysis**

445 All statistical analyses were performed with GraphPad Prism 5.0 software. One-way ANOVA
446 followed by Bonferroni´s post hoc test was used for the analysis of the luciferase reporter
447 assays and the DPI-ELISA.

448

449 ## Acknowledgments

450 We thank D. Thomas Rutkowski for providing *Atf6*$^{-/-}$ MEFs and Svenja Siebels for helpful
451 advice on the DPI-ELISA. This study was supported by the Deutsche
452 Forschungsgemeinschaft (BR 1730/6-1 to WB), the EU Horizon 2020 Marie Sklodowska-
453 Curie ITN-TREATMENT (Grant 721236 to BT), the German-Israeli Foundation (Grant I-1471-
454 414.13/2018 to BT), and Giovanni Armenise-Harvard Foundation (Career Development
455 Award to EvA).

456

457 ## Author contributions

458 Conceptualization, FH, BT, WB; Methodology, FH, EvA; Investigation, FH; Writing—Original
459 Draft, FH, WB; Writing—Review & Editing, FH, BT, WB; Funding Acquisition, WB;
460 Resources, EvA, BT; Supervision, WB.

461

462 ## Conflict of interest

463 The authors declare that they have no conflict of interest.

464

465 ## References

466 Alwine JC (2008) Modulation of host cell stress responses by human cytomegalovirus. *Curr*
467 *Top Microbiol Immunol* **325:** 263-279

468

469 Bakunts A, Orsi A, Vitale M, Cattaneo A, Lari F, Tade L, Sitia R, Raimondi A, Bachi A, van
470 Anken E (2017) Ratiometric sensing of BiP-client versus BiP levels by the unfolded protein
471 response determines its signaling amplitude. *Elife* **6**

472

473 Bhende PM, Dickerson SJ, Sun X, Feng WH, Kenney SC (2007) X-box-binding protein 1
474 activates lytic Epstein-Barr virus gene expression in combination with protein kinase D. *J*
475 *Virol* **81:** 7363-7370

476

477 Brand LH, Kirchler T, Hummel S, Chaban C, Wanke D (2010) DPI-ELISA: a fast and
478 versatile method to specify the binding of plant transcription factors to DNA in vitro. *Plant*
479 *methods* **6:** 25

480

481 Brune W, Ménard C, Heesemann J, Koszinowski UH (2001) A ribonucleotide reductase
482 homolog of cytomegalovirus and endothelial cell tropism. *Science* **291:** 303-305

483

484 Buchkovich NJ, Maguire TG, Yu Y, Paton AW, Paton JC, Alwine JC (2008) Human
485 cytomegalovirus specifically controls the levels of the endoplasmic reticulum chaperone
486 BiP/GRP78, which is required for virion assembly. *J Virol* **82:** 31-39

487

488 Buchkovich NJ, Yu Y, Pierciey FJ, Jr., Alwine JC (2010) Human cytomegalovirus induces the
489 endoplasmic reticulum chaperone BiP through increased transcription and activation of
490 translation by using the BiP internal ribosome entry site. *J Virol* **84:** 11479-11486

491 Byrd AE, Brewer JW (2012) Intricately Regulated: A Cellular Toolbox for Fine-Tuning XBP1
492 Expression and Activity. *Cells* **1:** 738-753

493

494 Calfon M, Zeng H, Urano F, Till JH, Hubbard SR, Harding HP, Clark SG, Ron D (2002) IRE1
495 couples endoplasmic reticulum load to secretory capacity by processing the XBP-1 mRNA.
496 *Nature* **415:** 92-96

497

498 Christianson JC, Ye Y (2014) Cleaning up in the endoplasmic reticulum: ubiquitin in charge.
499 *Nature structural & molecular biology* **21:** 325-335

500

501 Cohen N, Breker M, Bakunts A, Pesek K, Chas A, Argemi J, Orsi A, Gal L, Chuartzman S,
502 Wigelman Y, Jonas F, Walter P, Ernst R, Aragon T, van Anken E, Schuldiner M (2017) Iron
503 affects Ire1 clustering propensity and the amplitude of endoplasmic reticulum stress
504 signaling. *J Cell Sci* **130:** 3222-3233

505

506 Dolan A, Cunningham C, Hector RD, Hassan-Walker AF, Lee L, Addison C, Dargan DJ,
507 McGeoch DJ, Gatherer D, Emery VC, Griffiths PD, Sinzger C, McSharry BP, Wilkinson GW,
508 Davison AJ (2004) Genetic content of wild-type human cytomegalovirus. *J Gen Virol* **85:**
509 1301-1312

510

511 Drori A, Messerle M, Brune W, Tirosh B (2014) Lack of XBP-1 impedes murine
512 cytomegalovirus gene expression. *PLoS One* **9:** e110942

513

514 Harvey DM, Levine AJ (1991) p53 alteration is a common event in the spontaneous
515 immortalization of primary BALB/c murine embryo fibroblasts. *Genes Dev* **5:** 2375-2385

516

517 Isler JA, Skalet AH, Alwine JC (2005) Human cytomegalovirus infection activates and
518 regulates the unfolded protein response. *J Virol* **79:** 6890-6899

519

520 Kanemoto S, Kondo S, Ogata M, Murakami T, Urano F, Imaizumi K (2005) XBP1 activates
521 the transcription of its target genes via an ACGT core sequence under ER stress. *Biochem*
522 *Biophys Res Commun* **331:** 1146-1153

523

524 Lacaze P, Forster T, Ross A, Kerr LE, Salvo-Chirnside E, Lisnic VJ, Lopez-Campos GH,
525 Garcia-Ramirez JJ, Messerle M, Trgovcich J, Angulo A, Ghazal P (2011) Temporal profiling
526 of the coding and noncoding murine cytomegalovirus transcriptomes. *J Virol* **85:** 6065-6076

527

528 Lee K, Tirasophon W, Shen X, Michalak M, Prywes R, Okada T, Yoshida H, Mori K,
529 Kaufman RJ (2002) IRE1-mediated unconventional mRNA splicing and S2P-mediated ATF6

530 cleavage merge to regulate XBP1 in signaling the unfolded protein response. *Genes Dev* **16:**
531 452-466

532
533 Li H, Korennykh AV, Behrman SL, Walter P (2010) Mammalian endoplasmic reticulum stress
534 sensor IRE1 signals by dynamic clustering. *Proc Natl Acad Sci U S A* **107:** 16113-16118

535
536 Manzl C, Krumschnabel G, Bock F, Sohm B, Labi V, Baumgartner F, Logette E, Tschopp J,
537 Villunger A (2009) Caspase-2 activation in the absence of PIDDosome formation. *J Cell Biol*
538 **185:** 291-303

539
540 Marcinowski L, Lidschreiber M, Windhager L, Rieder M, Bosse JB, Radle B, Bonfert T, Gyory
541 I, de Graaf M, Prazeres da Costa O, Rosenstiel P, Friedel CC, Zimmer R, Ruzsics Z, Dolken
542 L (2012) Real-time transcriptional profiling of cellular and viral gene expression during lytic
543 cytomegalovirus infection. *PLoS Pathog* **8:** e1002908

544
545 Matar CG, Rangaswamy US, Wakeman BS, Iwakoshi N, Speck SH (2014) Murine
546 gammaherpesvirus 68 reactivation from B cells requires IRF4 but not XBP-1. *J Virol* **88:**
547 11600-11610

548
549 Maurel M, Chevet E, Tavernier J, Gerlo S (2014) Getting RIDD of RNA: IRE1 in cell fate
550 regulation. *Trends Biochem Sci* **39:** 245-254

551
552 Mocarski ES, Jr. (2002) Immunomodulation by cytomegaloviruses: manipulative strategies
553 beyond evasion. *Trends Microbiol* **10:** 332-339

554
555 Moore K, Hollien J (2015) Ire1-mediated decay in mammalian cells relies on mRNA
556 sequence, structure, and translational status. *Mol Biol Cell* **26:** 2873-2884

557
558 Navon A, Gatushkin A, Zelcbuch L, Shteingart S, Farago M, Hadar R, Tirosh B (2010) Direct
559 proteasome binding and subsequent degradation of unspliced XBP-1 prevent its intracellular
560 aggregation. *FEBS Lett* **584:** 67-73

561
562 Novoa I, Zeng H, Harding HP, Ron D (2001) Feedback inhibition of the unfolded protein
563 response by GADD34-mediated dephosphorylation of eIF2alpha. *J Cell Biol* **153:** 1011-1022

564
565 Qian Z, Xuan B, Chapa TJ, Gualberto N, Yu D (2012) Murine cytomegalovirus targets
566 transcription factor ATF4 to exploit the unfolded-protein response. *J Virol* **86:** 6712-6723

567
568 Reimold AM, Etkin A, Clauss I, Perkins A, Friend DS, Zhang J, Horton HF, Scott A, Orkin SH,
569 Byrne MC, Grusby MJ, Glimcher LH (2000) An essential role in liver development for
570 transcription factor XBP-1. *Genes Dev* **14:** 152-157

571
572 Ruegsegger U, Leber JH, Walter P (2001) Block of HAC1 mRNA translation by long-range
573 base pairing is released by cytoplasmic splicing upon induction of the unfolded protein
574 response. *Cell* **107:** 103-114

575 Smith MH, Ploegh HL, Weissman JS (2011) Road to ruin: targeting proteins for degradation
576 in the endoplasmic reticulum. *Science* **334:** 1086-1090

577
578 Stahl S, Burkhart JM, Hinte F, Tirosh B, Mohr H, Zahedi RP, Sickmann A, Ruzsics Z, Budt M,
579 Brune W (2013) Cytomegalovirus downregulates IRE1 to repress the unfolded protein
580 response. *PLoS Pathog* **9:** e1003544

581 Stern-Ginossar N, Weisburd B, Michalski A, Le VT, Hein MY, Huang SX, Ma M, Shen B,
582 Qian SB, Hengel H, Mann M, Ingolia NT, Weissman JS (2012) Decoding human
583 cytomegalovirus. *Science* **338:** 1088-1093

584
585 Sun CC, Thorley-Lawson DA (2007) Plasma cell-specific transcription factor XBP-1s binds to
586 and transactivates the Epstein-Barr virus BZLF1 promoter. *J Virol* **81:** 13566-13577

587
588 Swift S, Lorens J, Achacoso P, Nolan GP (2001) Rapid production of retroviruses for efficient
589 gene delivery to mammalian cells using 293T cell-based systems. *Curr Protoc Immunol*
590 **Chapter 10:** Unit 10 17C

591
592 Tirasophon W, Lee K, Callaghan B, Welihinda A, Kaufman RJ (2000) The endoribonuclease
593 activity of mammalian IRE1 autoregulates its mRNA and is required for the unfolded protein
594 response. *Genes Dev* **14:** 2725-2736

595
596 Tirosh B, Iwakoshi NN, Glimcher LH, Ploegh HL (2006) Rapid turnover of unspliced Xbp-1 as
597 a factor that modulates the unfolded protein response. *J Biol Chem* **281:** 5852-5860

598
599 Underwood KF, Mochin MT, Brusgard JL, Choe M, Gnatt A, Passaniti A (2013) A quantitative
600 assay to study protein:DNA interactions, discover transcriptional regulators of gene
601 expression, and identify novel anti-tumor agents. *Journal of visualized experiments : JoVE*

602
603 Urano F, Wang X, Bertolotti A, Zhang Y, Chung P, Harding HP, Ron D (2000) Coupling of
604 stress in the ER to activation of JNK protein kinases by transmembrane protein kinase IRE1.
605 *Science* **287:** 664-666

606
607 van Diemen FR, Kruse EM, Hooykaas MJ, Bruggeling CE, Schurch AC, van Ham PM, Imhof
608 SM, Nijhuis M, Wiertz EJ, Lebbink RJ (2016) CRISPR/Cas9-Mediated Genome Editing of
609 Herpesviruses Limits Productive and Latent Infections. *PLoS Pathog* **12:** e1005701

610
611 Walter P, Ron D (2011) The unfolded protein response: from stress pathway to homeostatic
612 regulation. *Science* **334:** 1081-1086

613
614 Wang Y, Shen J, Arenzana N, Tirasophon W, Kaufman RJ, Prywes R (2000) Activation of
615 ATF6 and an ATF6 DNA binding site by the endoplasmic reticulum stress response. *J Biol*
616 *Chem* **275:** 27013-27020

617
618
619

620 Wilson SJ, Tsao EH, Webb BL, Ye H, Dalton-Griffin L, Tsantoulas C, Gale CV, Du MQ,
621 Whitehouse A, Kellam P (2007) X box binding protein XBP-1s transactivates the Kaposi's
622 sarcoma-associated herpesvirus (KSHV) ORF50 promoter, linking plasma cell differentiation
623 to KSHV reactivation from latency. *J Virol* **81:** 13578-13586

624

625 Wu J, Rutkowski DT, Dubois M, Swathirajan J, Saunders T, Wang J, Song B, Yau GD,
626 Kaufman RJ (2007) ATF6alpha optimizes long-term endoplasmic reticulum function to
627 protect cells from chronic stress. *Dev Cell* **13:** 351-364

628

629 Yoshida H, Haze K, Yanagi H, Yura T, Mori K (1998) Identification of the cis-acting
630 endoplasmic reticulum stress response element responsible for transcriptional induction of
631 mammalian glucose-regulated proteins. Involvement of basic leucine zipper transcription
632 factors. *J Biol Chem* **273:** 33741-33749

633

634 Yoshida H, Matsui T, Yamamoto A, Okada T, Mori K (2001) XBP1 mRNA is induced by
635 ATF6 and spliced by IRE1 in response to ER stress to produce a highly active transcription
636 factor. *Cell* **107:** 881-891

637

638 Yoshida H, Oku M, Suzuki M, Mori K (2006) pXBP1(U) encoded in XBP1 pre-mRNA
639 negatively regulates unfolded protein response activator pXBP1(S) in mammalian ER stress
640 response. *J Cell Biol* **172:** 565-575

641

642 Yoshida H, Uemura A, Mori K (2009) pXBP1(U), a negative regulator of the unfolded protein
643 response activator pXBP1(S), targets ATF6 but not ATF4 in proteasome-mediated
644 degradation. *Cell structure and function* **34:** 1-10

645

646 Yu F, Feng J, Harada JN, Chanda SK, Kenney SC, Sun R (2007) B cell terminal
647 differentiation factor XBP-1 induces reactivation of Kaposi's sarcoma-associated herpesvirus.
648 *FEBS Lett* **581:** 3485-3488

649

650 Yu Y, Pierciey FJ, Jr., Maguire TG, Alwine JC (2013) PKR-like endoplasmic reticulum kinase
651 is necessary for lipogenic activation during HCMV infection. *PLoS Pathog* **9:** e1003266

652

653 Zhang L, Wang A (2012) Virus-induced ER stress and the unfolded protein response. *Front*
654 *Plant Sci* **3:** 293

655

656 Zhao Y, Li X, Ma K, Yang J, Zhou J, Fu W, Wei F, Wang L, Zhu WG (2013) The axis of
657 MAPK1/3-XBP1u-FOXO1 controls autophagic dynamics in cancer cells. *Autophagy* **9:** 794-
658 796

659

660 Zhou Y, Lee J, Reno CM, Sun C, Park SW, Chung J, Fisher SJ, White MF, Biddinger SB,
661 Ozcan U (2011) Regulation of glucose homeostasis through a XBP-1-FoxO1 interaction. *Nat*
662 *Med* **17:** 356-365

663

664

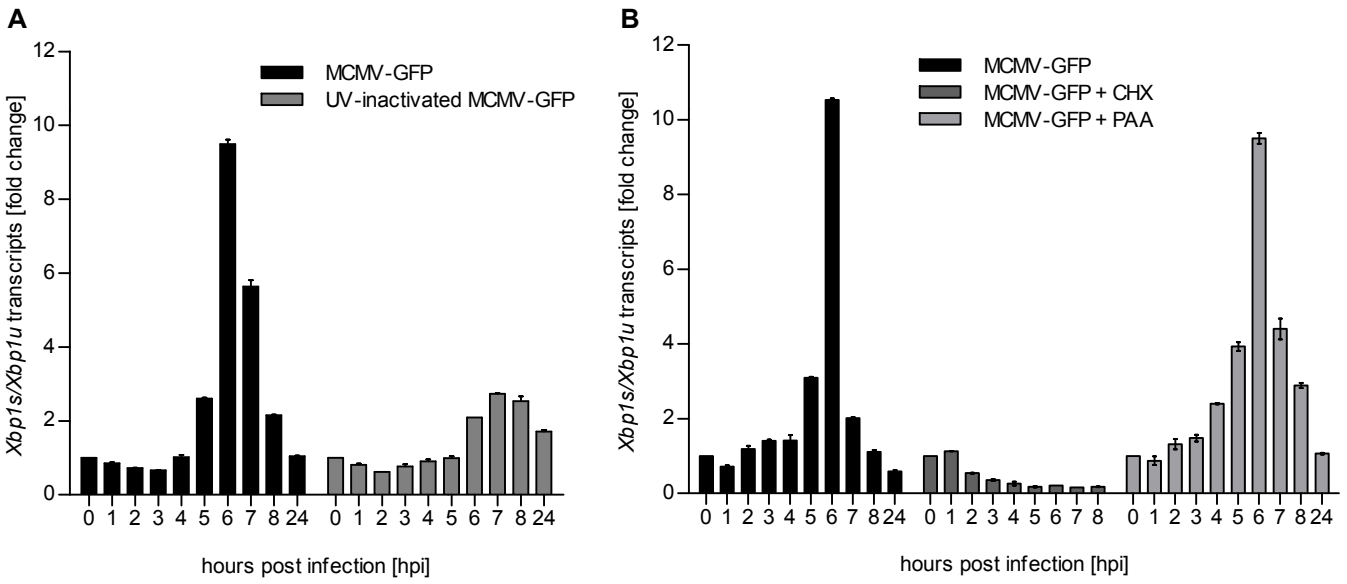

Figure 1.
MCMV induces *Xbp1s* mRNA splicing at early time of infection

A. MEFs were infected with MCMV-GFP or UV-inactivated MCMV-GFP (MOI 4). Cells were harvested at the indicated times, total RNA was extracted, and *Xbp1s* and *Xbp1u* transcripts were quantified by qPCR. Changes in the *Xbp1s/Xbp1u* ratio relative to uninfected cells are plotted as bar diagram (means ±SEM of 3 biological replicates).

B. MEFs were infected with MCMV-GFP as described above and treated with vector, CHX (50µg/ml) or PAA (250ng/ml). Changes in the *Xbp1s/Xbp1u* ratio were determined as described above.

Data provided in Figure 1 – source data 1

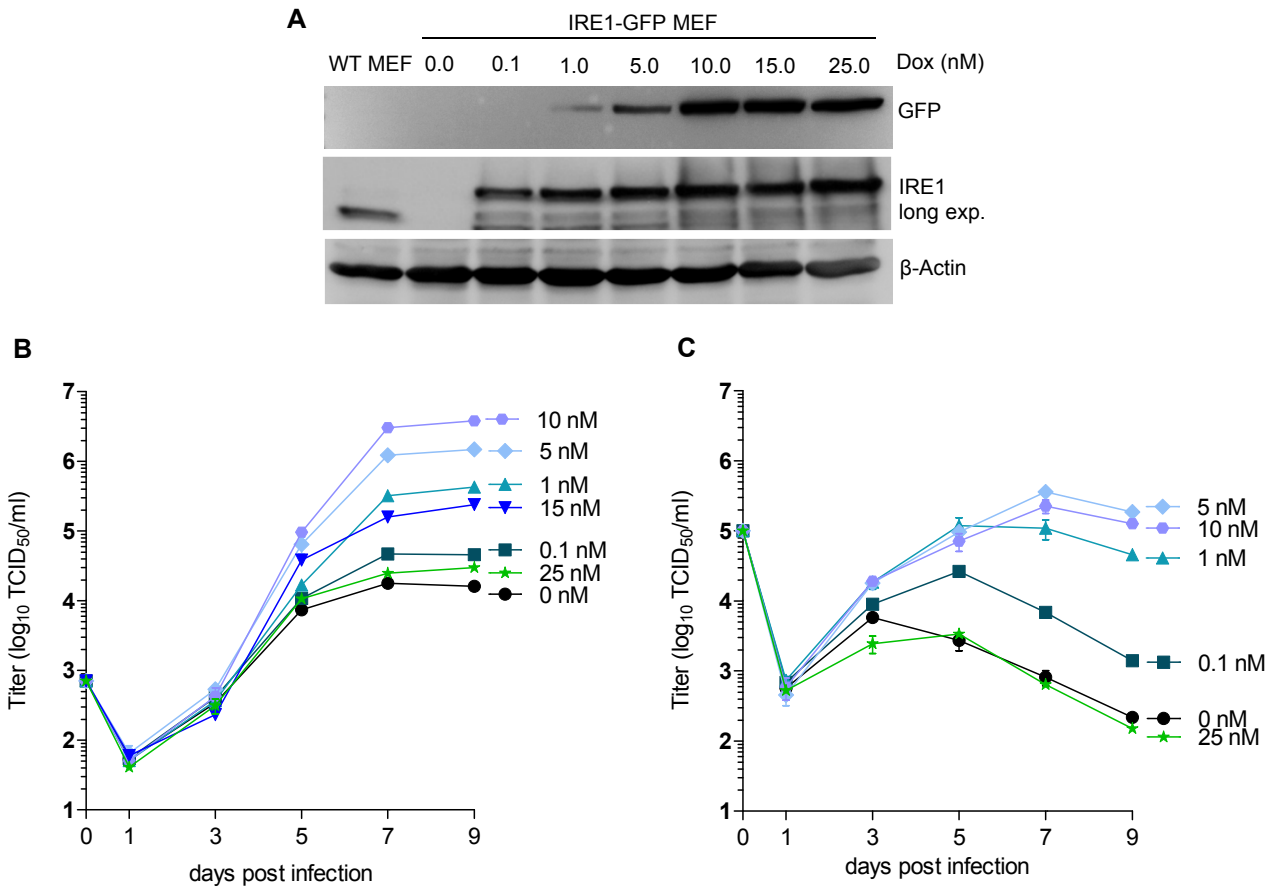

Figure 2.
Moderate IRE1 expression is beneficial for MCMV replication.

A. Immunoblot analysis of *Ire1*$^{-/-}$ MEFs expressing IRE1-GFP in a doxycycline (dox)-inducible manner. Cells were treated with different dox concentrations for 24 h. IRE1-GFP expression was detected with GFP or IRE1-specific antibodies. Endogenous IRE1 levels in WT MEFs were detected only with the IRE1-specific antibody. The immunoblot is representative of 3 independent experiments.

B. Multistep MCMV replication kinetics on IRE1-GFP MEFs induced with different dox concentrations. 24 h after induction, cells were infected with MCMV-GFP (MOI 0.1). Virus titers in the supernatants were determined by titration and are shown as means ±SEM of 3 biological replicates.

C. Single step MCMV replication kinetics on IRE1-GFP MEFs induced with dox as above, infected with MCMV-GFP (MOI 3) and are shown as means ±SEM of 3 biological replicates.

Data provided in Figure 2 – source data 1.

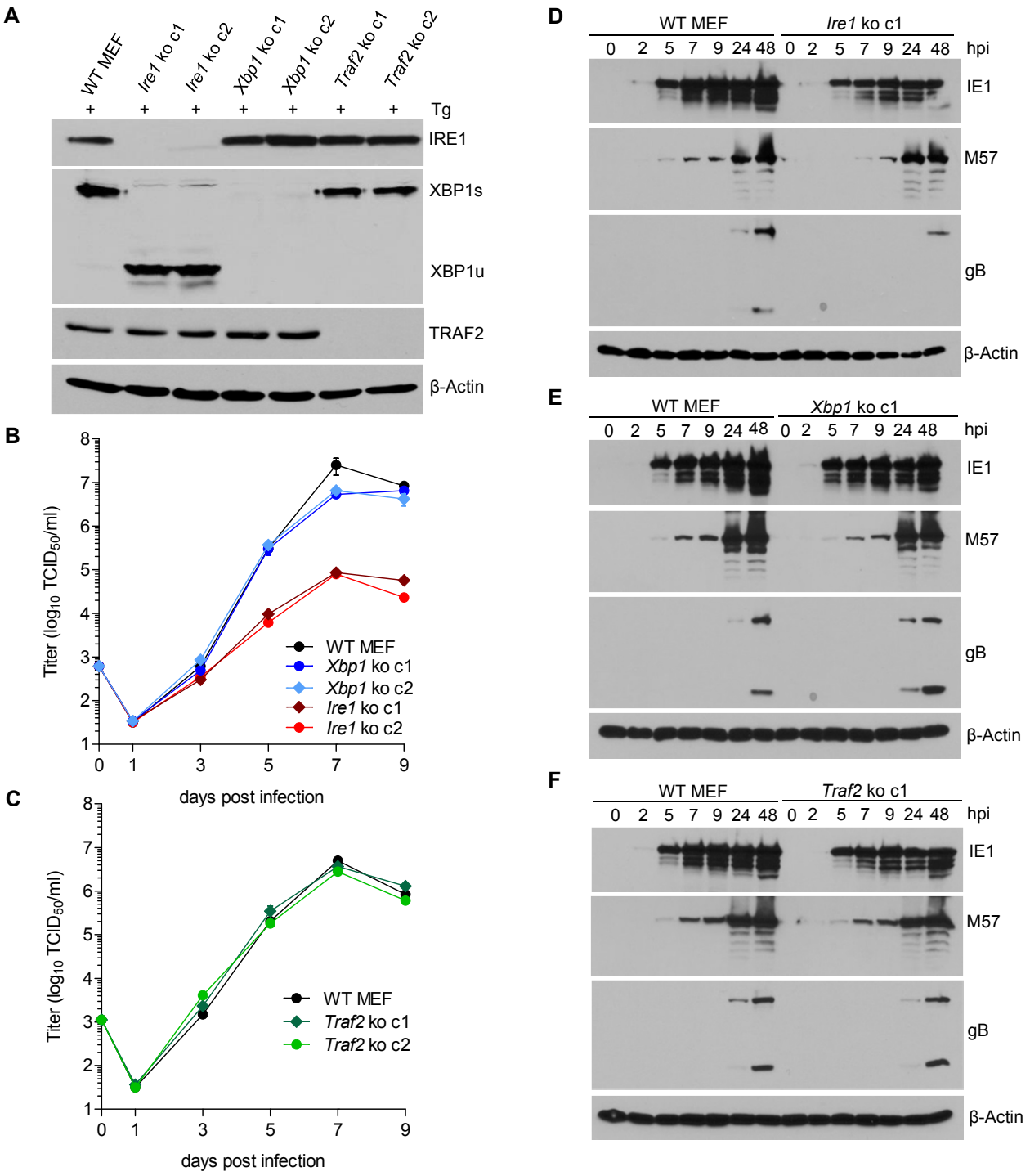

Figure 3.

IRE1, but not XBP1 or TRAF2, is required for efficient MCMV replication and viral protein expression

A. Immunoblot analysis of *Ire1*, *Xbp1* and *Traf2* ko cell lines. Two ko clones were generated for each gene by CRISPR/Cas9 gene editing using different gRNAs. Cells were treated for 4 h with Thapsigargin (Tg) to induce *Xbp1* mRNA splicing and to increase XBP1 expression.

B,C. Multistep MCMV replication kinetics in *Ire1*, *Xbp1* and *Traf2 ko* cells, respectively. Cells were infected with MCMV-GFP (MOI 0.1) Virus titers in the supernatants were determined by titration and are shown as means ±SEM of 3 biological replicates.

D-F. Immunoblot analysis of viral protein expression kinetics in *Ire1*, *Xbp1* and *Traf2 ko* cells, respectively. Cells were infected with MCMV-GFP (MOI 3) and harvested at different times post infection. Expression levels of the viral immediate-early 1 (IE1) protein, the major DNA binding protein (M57; an early protein), and glycoprotein B (gB; a late protein) were detected with specific antibodies, β-Actin served as loading control.

Immunoblots are representative of 2 independent experiments. Data provided in Figure 3 – source data 1.

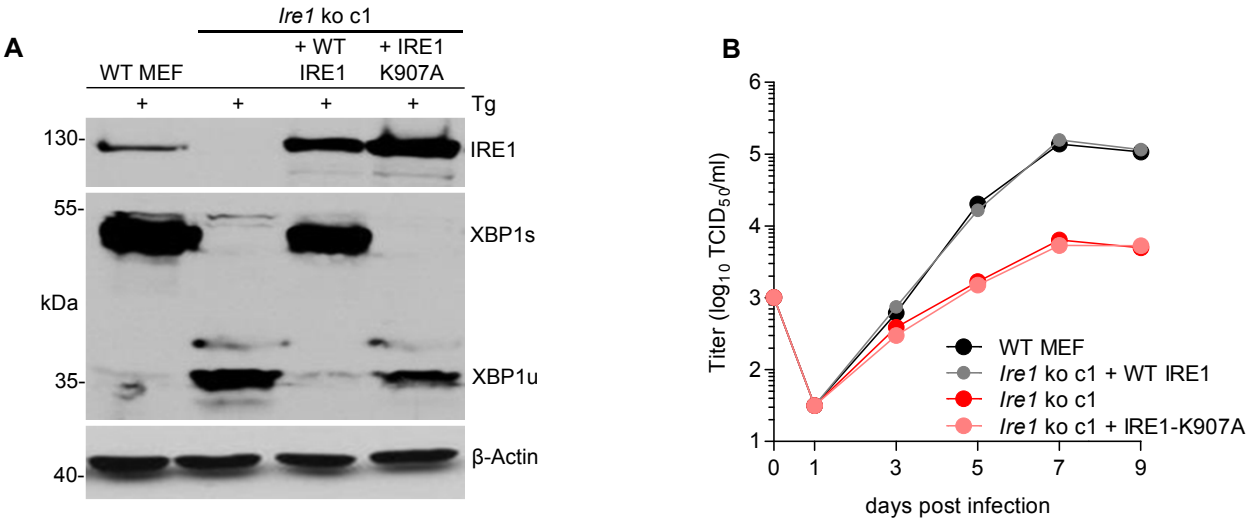

Figure 4.
The RNase function of IRE1 is required for efficient MCMV replication.

A. Immunoblot analysis of *Ire1* ko *c1* transduced with retroviral vectors expressing WT IRE1 or IRE1-K907A (RNase-dead). Cells were treated for 4 h with Thapsigargin (Tg) to induce *Xbp1* mRNA splicing and to increase XBP1 expression. IRE1 and XBP1 protein expression was detected by immunoblot (representative of 2 independent experiments).

B. Multistep MCMV replication kinetics in *Ire1 ko* cells complemented with WT IRE1 or IRE1-K907A, respectively. Cells were infected with MCMV-GFP (MOI 0.1). Virus titers in the supernatants were determined by titration and are shown as means ±SEM of 3 biological replicates.

Data provided in Figure 4 – source data 1.

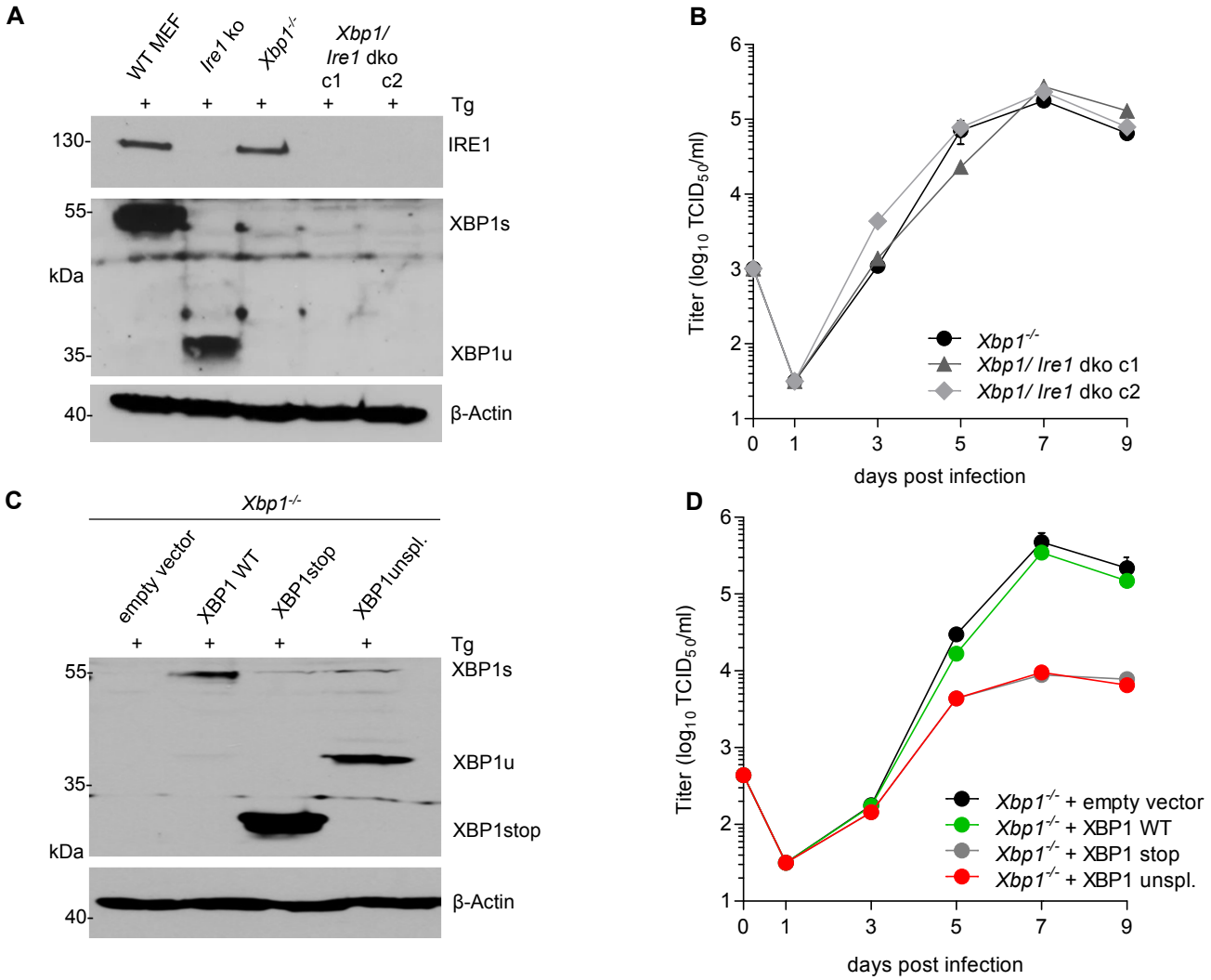

Figure 5.
XBP1u acts as a repressor for MCMV replication.

A. *Xbp1*$^{-/-}$ MEFs were used to knock out *Ire1* by CRISPR/Cas9 gene editing. Two double ko (dko) cell clones were generated with different gRNAs. IRE1 and XBP1 protein expression in the two dko clones and control cells was detected by immunoblot analysis. Cells were treated for 4 h with Thapsigargin (Tg) to induce *Xbp1* mRNA splicing and to increase XBP1 expression.

B. Multistep MCMV replication kinetics in *Xbp1*$^{-/-}$ and *Xbp1/Ire1* dko MEFs. Cells were infected with MCMV-GFP (MOI 0.1) Virus titers in the supernatants were determined by titration and are shown as means ±SEM of 3 biological replicates.

C. Immunoblot analysis of *Xbp1*$^{-/-}$ MEF transduced with retroviral vectors expressing a WT (spliceable) *Xbp1* transcript, an unspliceable *Xbp1* transcript, or a truncated (*Xbp1*stop) transcript. Cells were treated with Tg as described in A.

D. Multistep MCMV replication kinetics in cells shown in C. Infection and titration was done as in B.

Immunoblots are representative of 2 independent experiments. Data provided in Figure 5 – source data 1

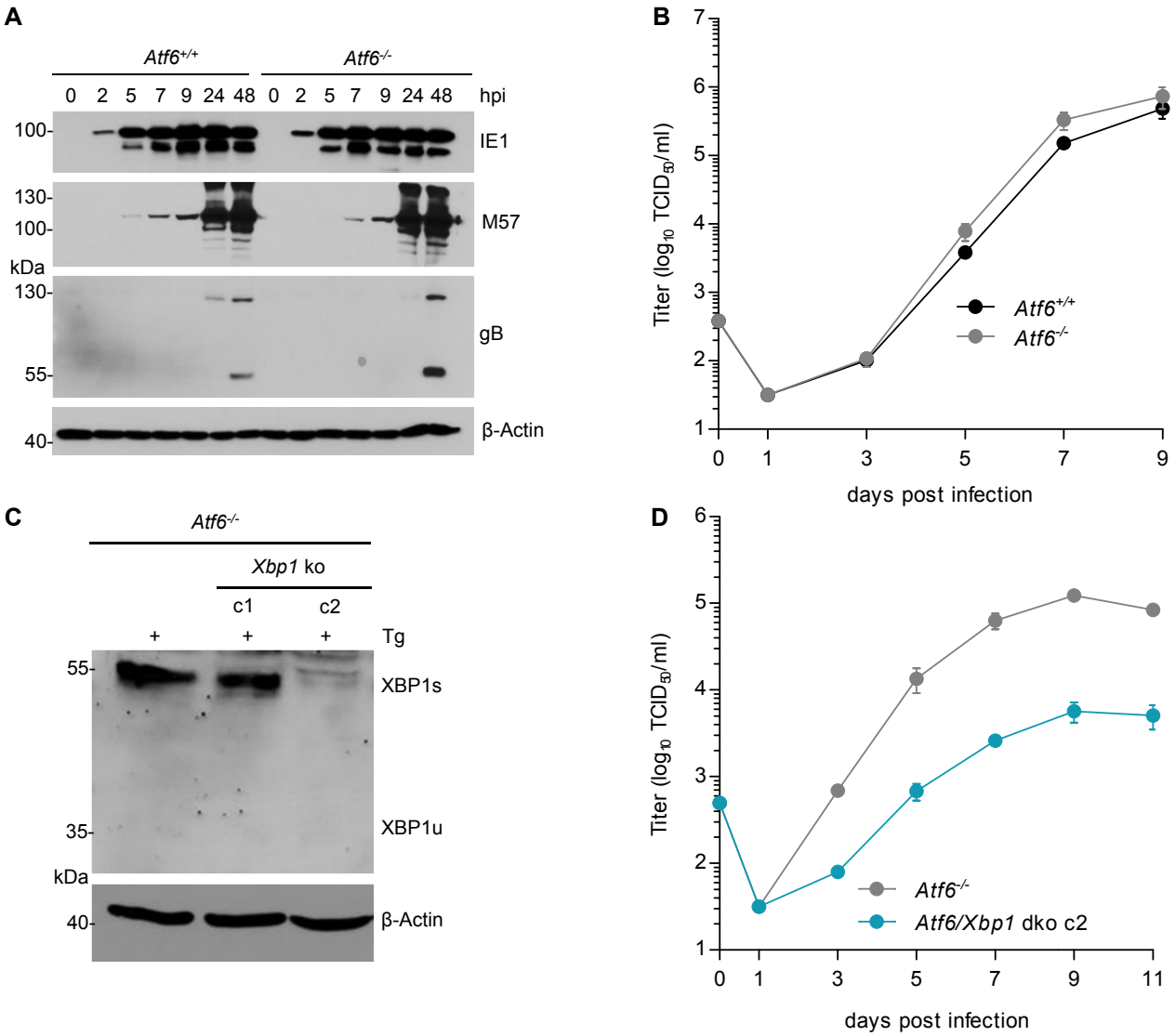

Figure 6.
MCMV replication is impaired in cells lacking *Atf6* and *Xbp1*.

A. Immunoblot analysis of viral gene expression of *Atf6*$^{+/+}$ and *Atf6*$^{-/-}$ cells infected with MCMV-GFP at an MOI of 3 $TCID_{50}$/ml. At indicated times cells were lysed and stained for the immediate-early 1 protein (IE1), the major DNA binding protein (M57; early gene) and glycoprotein B (gB; late gene) by immunoblot. β-Actin served as loading control.

B. Multistep replication kinetics. *Atf6*$^{+/+}$ and *Atf6*$^{-/-}$ cells were infected with MCMV-GFP at an MOI of 0.1 $TCID_{50}$/ml. Virus titers in the supernatants were determined by titration and are shown as means ±SEM of 3 biological replicates.

C. Knockout of *Xbp1* in *Atf6*$^{-/-}$ cells using CRISPR/Cas9 gene editing. Two single cell clones generated by two individual gRNAs (c1 and c2) were analyzed for XBP1s and XBP1u expression by immunoblot. 4h prior to harvesting, cells were stimulated with thapsigargin (Tg) to enhance XBP1 expression. The parental *Atf6*$^{-/-}$ cells are shown as control.

D. Multistep replication kinetics of *Atf6*/*Xbp1* dko cells (clone c2). MCMV infection and titration was done as described in B.

Immunoblots are representative of 2 independent experiments. Data provided in Figure 6 – source data 1

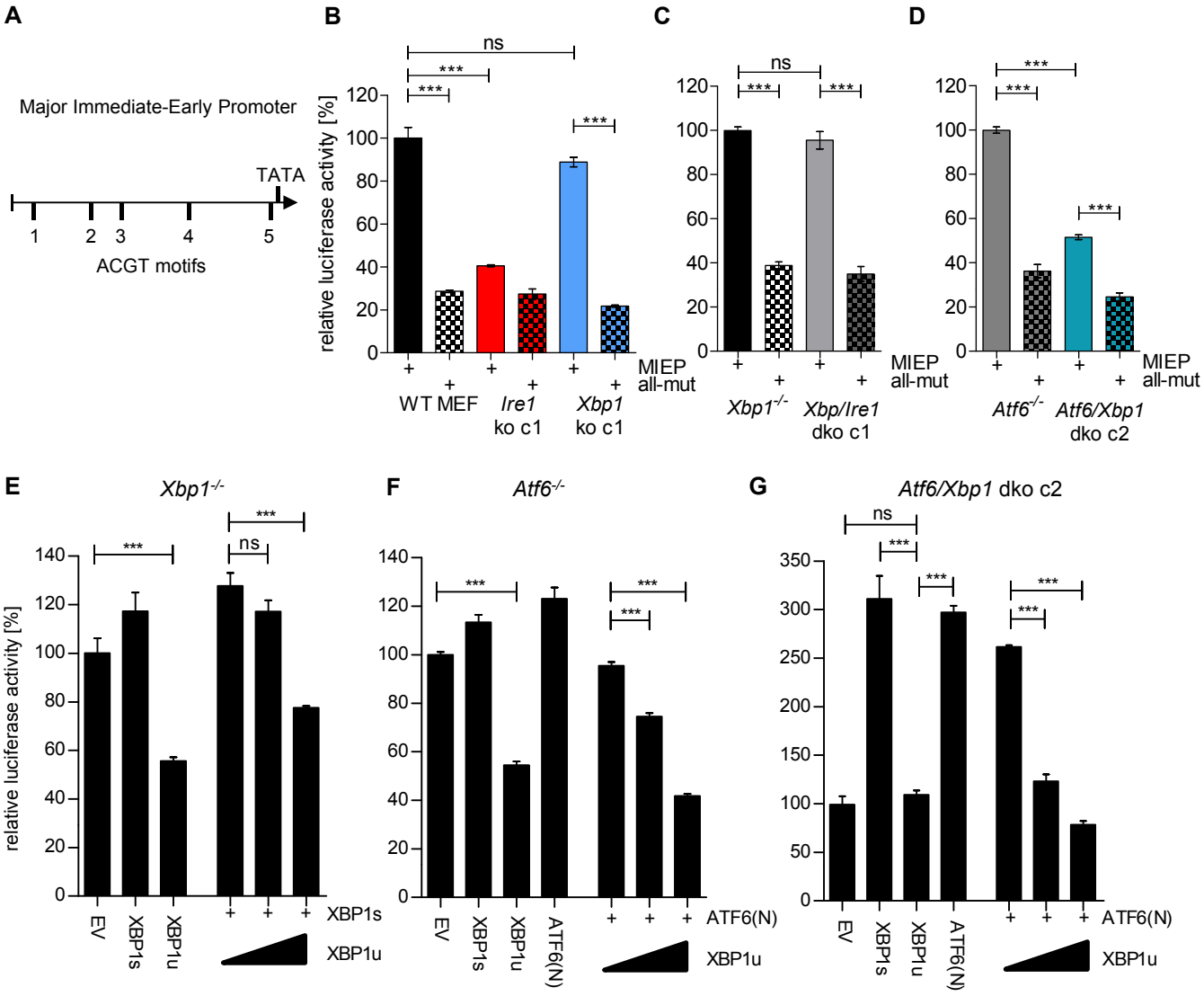

Figure 7. XBP1s and ATF6-mediated activation of the MCMV MIEP is repressed by XBP1u.

A. Schematic representation of the MCMV Major Immediate-Early Promoter (MIEP) with TATA box and 5 ACGT motifs.

B. WT MEFs, *Ire1* ko and *Xbp1* ko cells were transfected with a firefly luciferase vector containing either the WT major immediate-early promotor (MIEP) or a MIEP with 5 mutated ACGT motifs (all-mut). Renilla luciferase was expressed by co-transfection and used for normalization. Relative luciferase activities (firefly : renilla) ±SEM of at least 3 biological replicates are shown. ***, $p<0.001$; ns, not significant, $p>0.05$.

C. *Xbp1*$^{-/-}$ and *Xbp1/Ire1* dko cells were transfected as in B and the relative luciferase activity was determined.

D. *Atf6*$^{-/-}$ and *Atf6/Xbp1* dko cells were transfected as in B and the relative luciferase activity was determined.

E. *Xbp1*$^{-/-}$ MEFs were co-transfected with firefly and renilla luciferase vectors as in B. Expression vectors for XBP1s, XBP1u, ATF6(N), or empty vector (EV) were co-transfected. Relative luciferase activities (firefly : renilla) ±SEM of 3 biological replicates are shown.

F. *Atf6*$^{-/-}$ cells were transfected as in E and the relative luciferase activity was determined.

G. *Atf6/Xbp1* dko cells were transfected as in E and the relative luciferase activity was determined.

Data provided in Figure 7 – source data 1

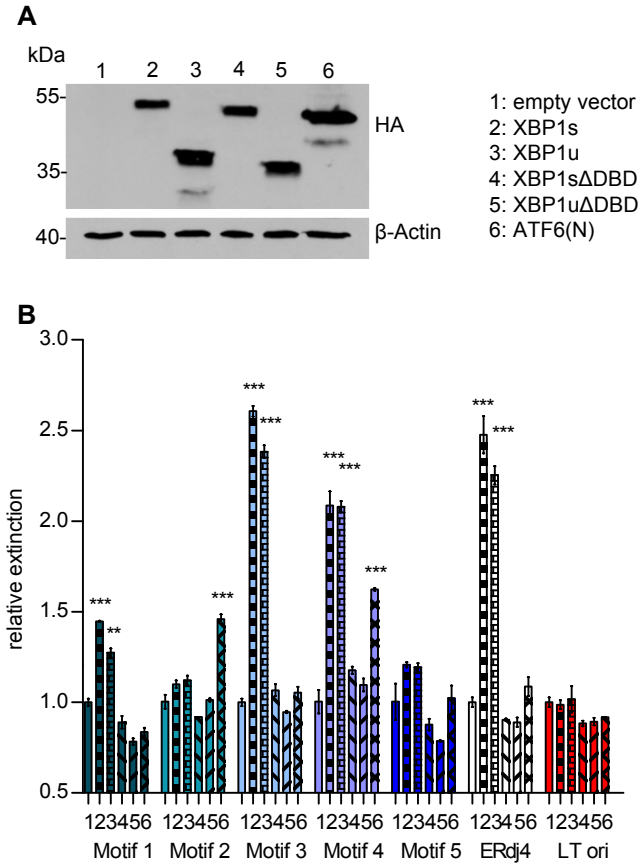

Figure 8. Transcription factor binding the MIE promotor

A. HEK 293A cells were transfected with expression vectors encoding HA-tagged WT or mutant XBP1 and ATF6(N) transcription factors. Nuclear extracts were obtained, and transcription factor expression was verified by immunoblot analysis (representative of 2 independent experiments).

B. Microtiter plates coated with dsDNA oligonucleotides containing XBP1 core binding motifs from the MCMV major immediate-early promoter, the ERdj4 promoter (positive control) or an unrelated sequence from the SV40 origin of replication (negative control). Wells were incubated with nuclear extracts 1 to 6 shown in A, and transcription factor binding was measured by DPI-ELISA, and values were normalized to extract 1 (empty vector). Means ±SEM of 3 biological replicates are shown. Significance was determined for all values above the cut-off (1.25). **, $p<0.01$; ***, $p<0.001$.

Data provided in Figure 8 – source data 1

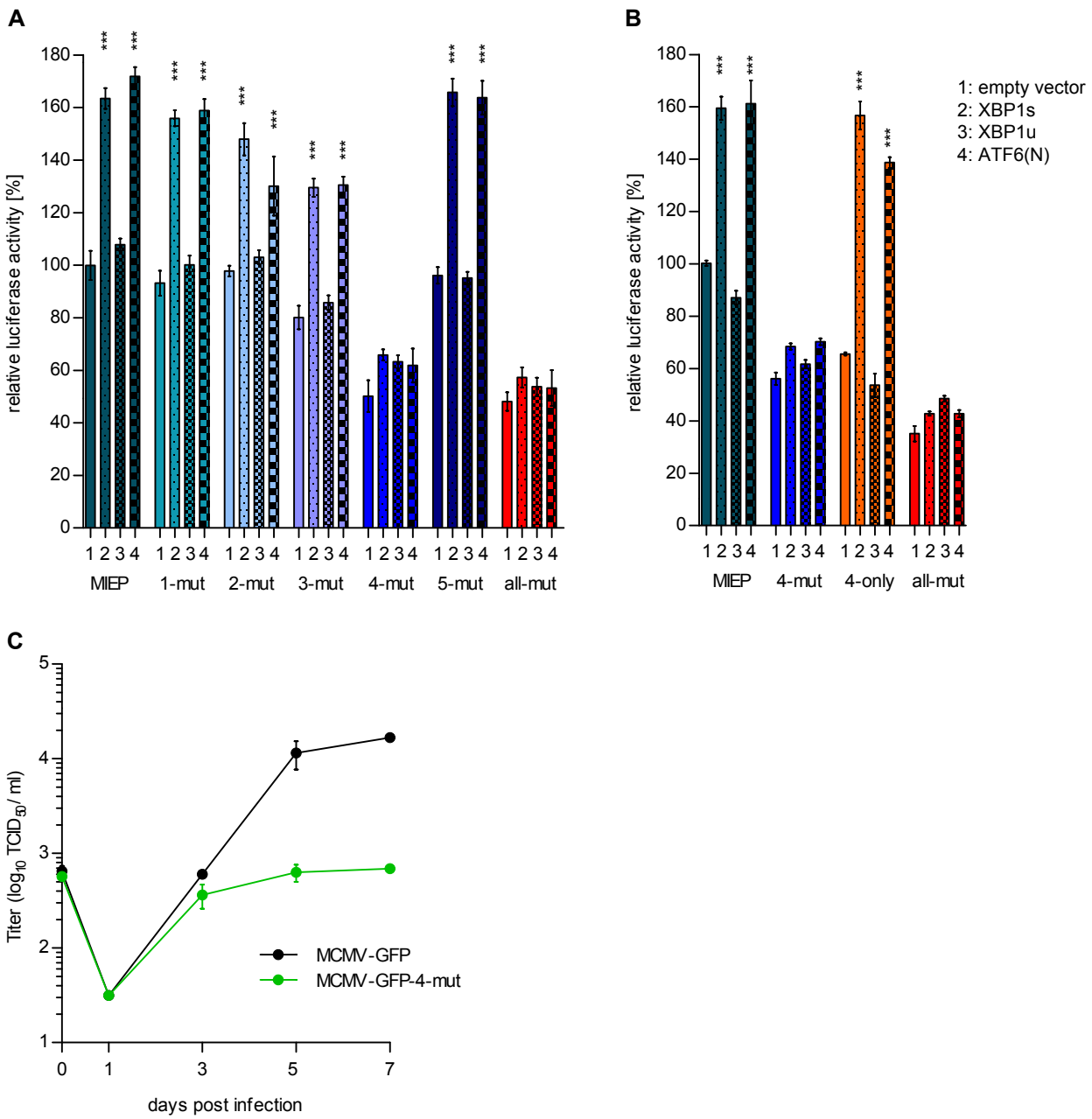

Figure 9. Motif 4 is necessary and sufficient for MIEP activation by XBP1s and ATF6(N).

A *Atf6/Xbp1* dko MEFs cells were transfected with a firefly luciferase vector containing either the WT major immediate-early promotor (MIEP) or a MIEP with 1 or all ACGT motifs mutated. Expression vectors for XBP1a, XBP1u, ATF6(N), or empty vector (EV) were co-transfected. Renilla luciferase was expressed by co-transfection and used for normalization. Relative luciferase activities (firefly : renilla) ±SEM of 3 biological replicates are shown. ***, $p<0.001$; all other differences were not significant ($p>0.05$).

B *Atf6/Xbp1* dko MEF cells were transfected and analyzed as in A. In addition, a MIEP vector with all ACGT motifs mutated except motif 4 (4-only) was included.

C Multistep MCMV replication kinetics in WT MEF cells. Cells were infected with MCMV-GFP or MCMV-GFP-4-mut (MOI 0.1), respectively. Virus titers in the supernatants were determined by titration and are shown as means ±SEM of 3 biological replicates.

Data provided in Figure 9 – source data 1